Supplementary Materials

Thiazolidine-Based Fluorescent Chiral Ionic Liquids for Trace Copper(II) Ion Sensing

Cassiana H. Griebeler [1], Mariana F. Bach [2], Henrique C. Silva, Jr. [1], Fabiano S. Rodembusch [1,*], Felipe L. Coelho [3,*] and Paulo H. Schneider [1,*]

[1] Instituto de Química, Laboratory of Molecular Catalysis (LAMOCA), Universidade Federal do Rio Grande do Sul (UFRGS), P.O. Box 15003, Porto Alegre 91501-970, RS, Brazil
[2] Instituto Federal Farroupilha, Campus Alegrete, Rodovia RS-377, Alegrete 97555-000, RS, Brazil
[3] Instituto de Química, Universidade Federal de Goiás (UFG), Campus Samambaia, Goiânia 74690-900, GO, Brazil
* Correspondence: rodembusch@iq.ufrgs.br (F.S.R.); felipecoelho@ufg.br (F.L.C.); paulos@iq.ufrgs.br (P.H.S.)

Table of Contents

Experimental Procedures

Synthesis of precursor **2**: A round-bottomed flask was charged with L-cysteine chlorhydrate (16 g, 95 mmol), distilled water (10 mL), and formaldehyde 37% (11 mL). The mixture was stirred for 24 h at room temperature. Then, ethyl alcohol (25 mL) and pyridine were added. The precipitate was filtered and washed with ethyl alcohol (5 x 20 mL). The product was obtained as a white solid powder with no additional purification needed. Yield: 80 %. Melting point: 180°C (decomposition). ^{1}H NMR (400 MHz, $CDCl_3$) δ: 4.19 (d, *J* = 8.9 Hz, 1H); 4.00 (d, *J* = 8.9 Hz, 1H); 3,81 (t, *J* = 6.8 Hz, 1H); 3.05 (dd, *J* = 7.1 Hz and 10.1, 1H); 2.79 (dd, *J* = 6.6 Hz and 10.1 Hz, 1H).

Synthesis of precursor ***3***: A round-bottomed flask was charged with compound **2** (10.8 g, 81 mmol), 1,4-dioxane (162 mL), distilled water (81 mL), and NaOH aqueous solution (1.0 $mol \cdot L^{-1}$, 81 mL). The system was cooled to 0°C and Boc_2O (19.42 g, 89 mmol) was added. The mixture was then kept at room temperature and stirred for 12 h. The mixture was concentrated under a vacuum, cooled to 0°C, and AcOEt (80 mL) was added. The acidification was carried out until pH 2-3 through the addition of $KHSO_4$ 1.0 $mol \cdot L^{-1}$ aqueous solution drops. The aqueous layer was extracted with ethyl acetate (3 x 60 mL). The organic layer was combined, washed with distilled water, dried with $MgSO_4$, and the solvent was evaporated. The product was obtained as a white solid powder. Yield: 90 %. ^{1}H NMR (400 MHz, $CDCl_3$, mixture of conformers) δ: 7.86-7.40 (m, 1H); 4.94-4.68 (m, 1H); 4.68-4.54 (m, 1H); 4.53-4.33 (m, 1H); 3.46-3.22 (2H); 1.49 (s, 9H).

Spectroscopic Characterization

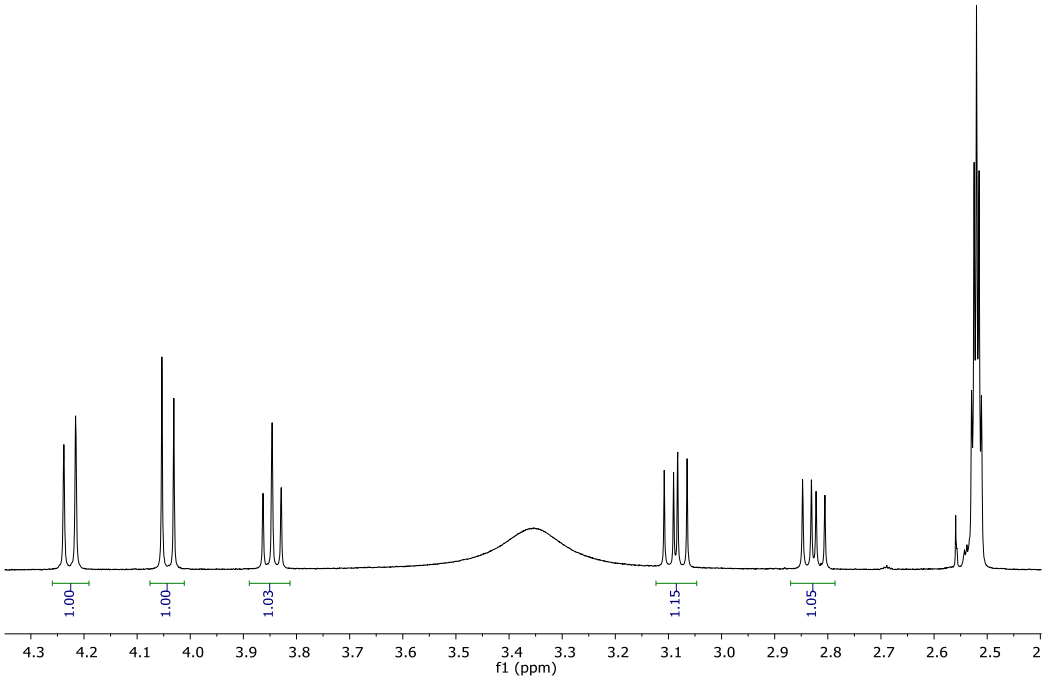

Figure S1. ^{1}H NMR spectrum (DMSO-d_6, 400 MHz) of compound **2**.

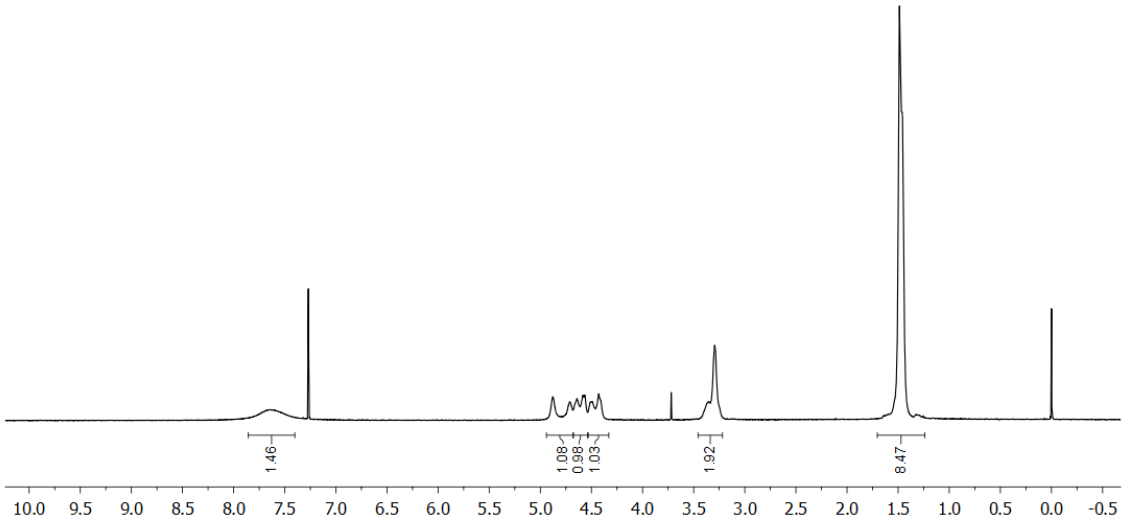

Figure S2. ^{1}H NMR spectrum ($CDCl_3$, 400 MHz) of compound **3**.

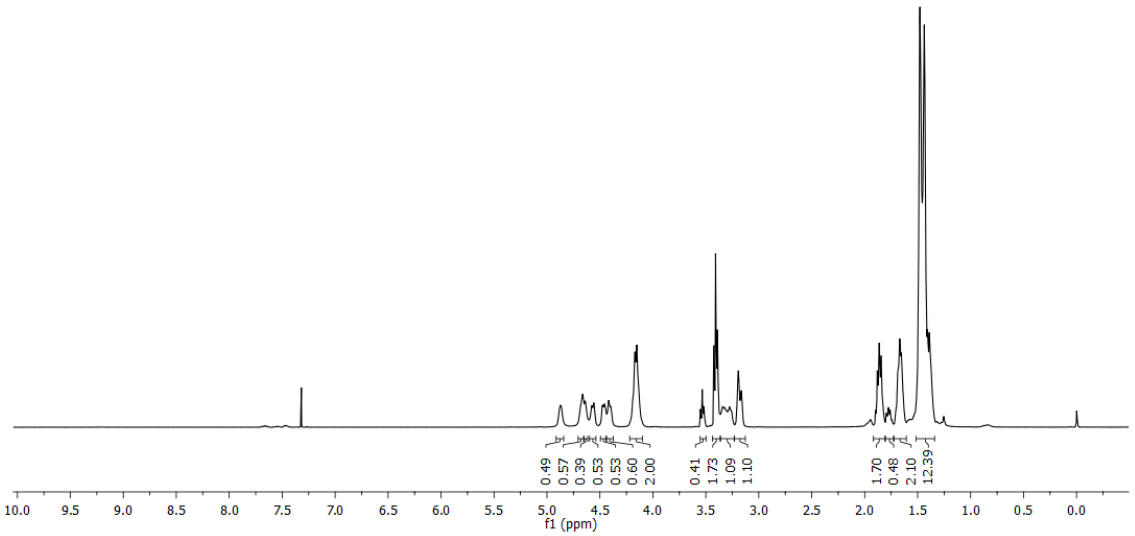

Figure S3. ^{1}H NMR spectrum ($CDCl_3$, 400 MHz) of compound **4**.

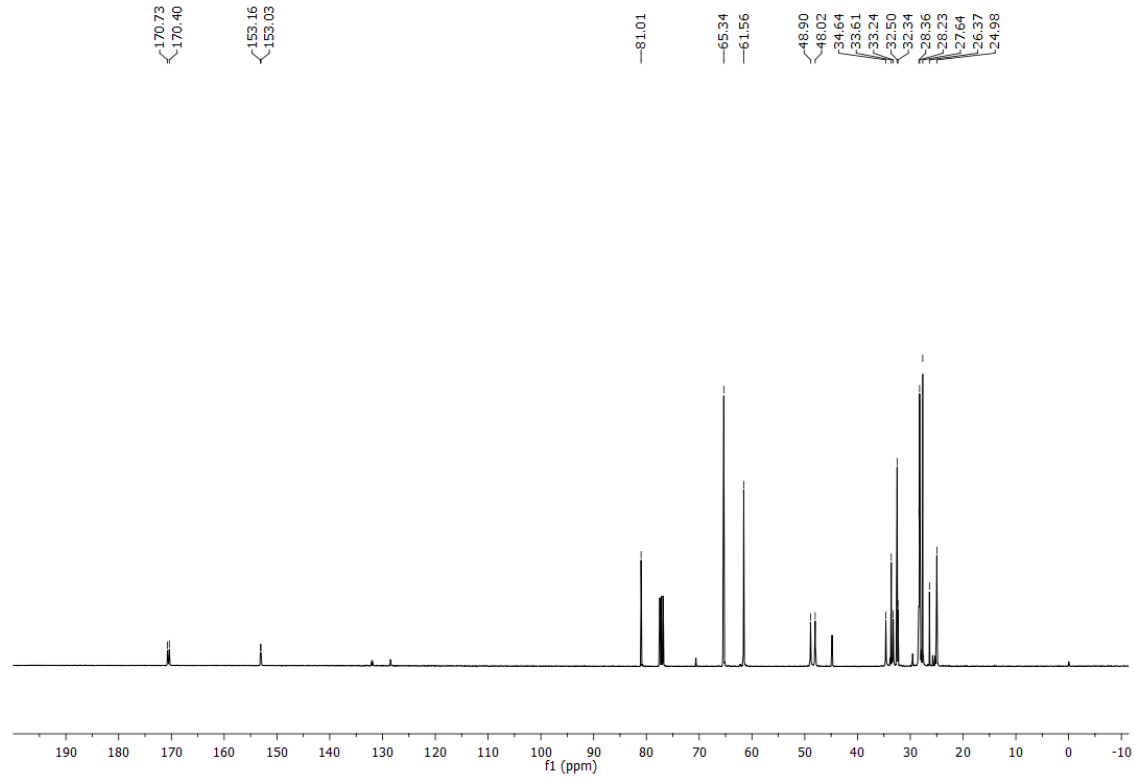

Figure S4. ^{13}C NMR spectrum ($CDCl_3$, 100 MHz) of compound **4**.

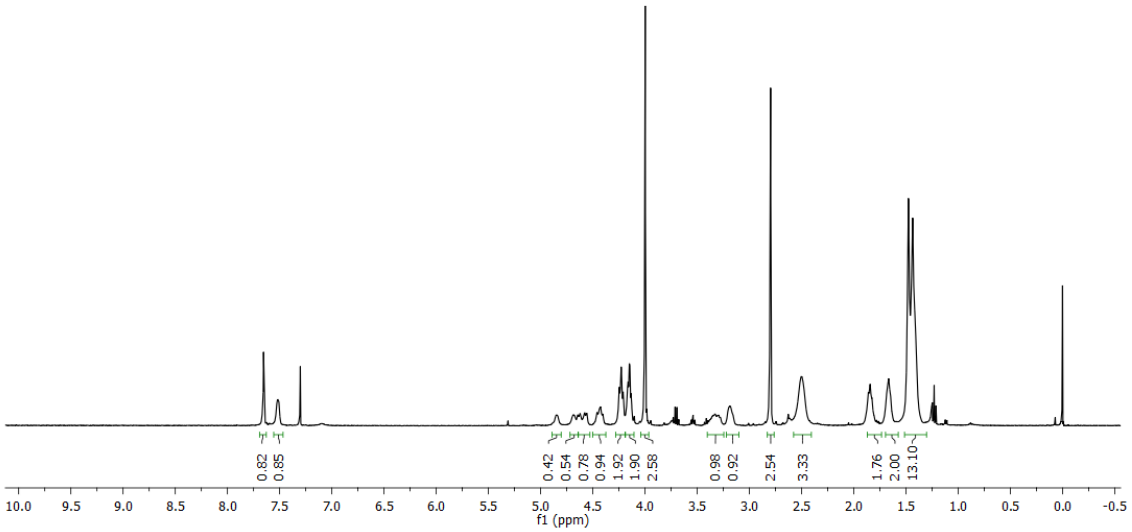

Figure S5. ^{1}H NMR spectrum ($CDCl_3$, 400 MHz) of compound **5a**.

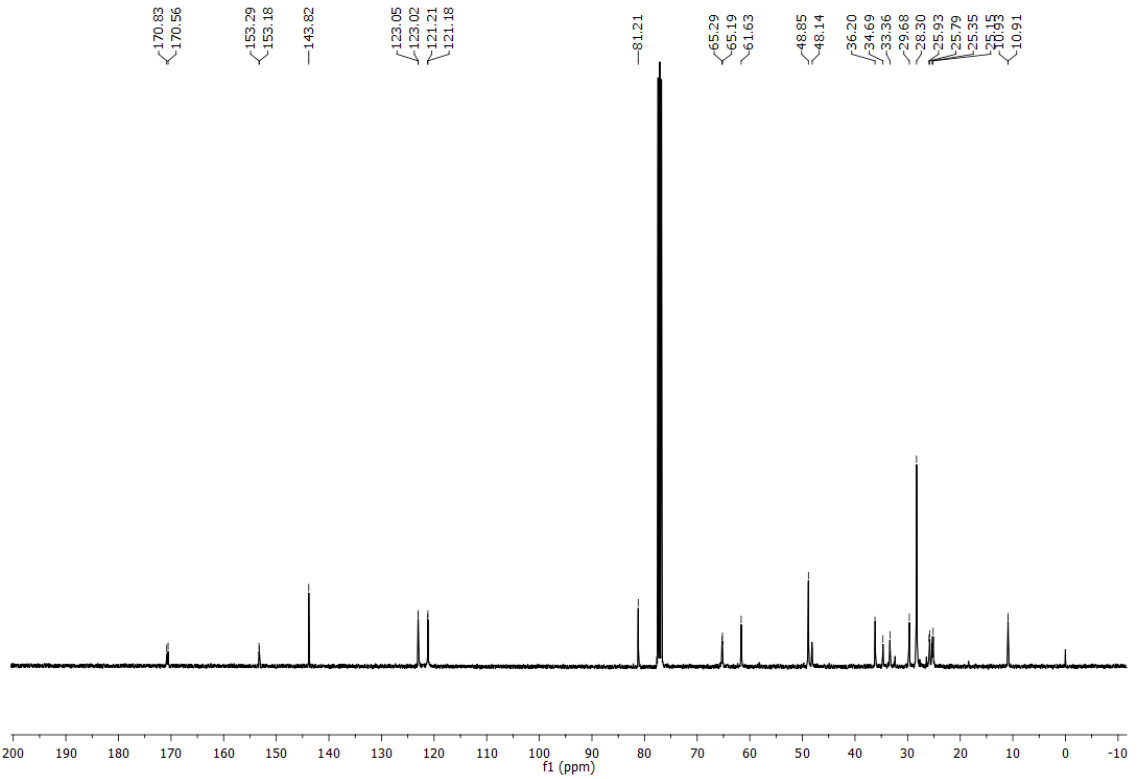

Figure S6. ^{13}C NMR spectrum ($CDCl_3$, 100 MHz) of compound **5a**.

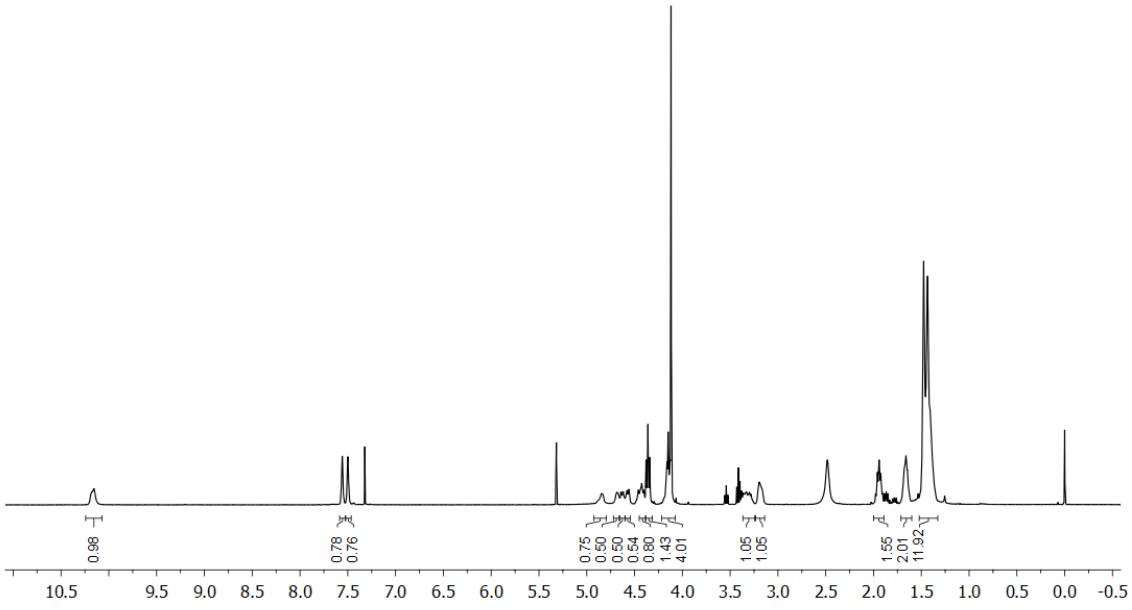

Figure S7. ^{1}H NMR spectrum ($CDCl_3$, 400 MHz) of compound **5b**.

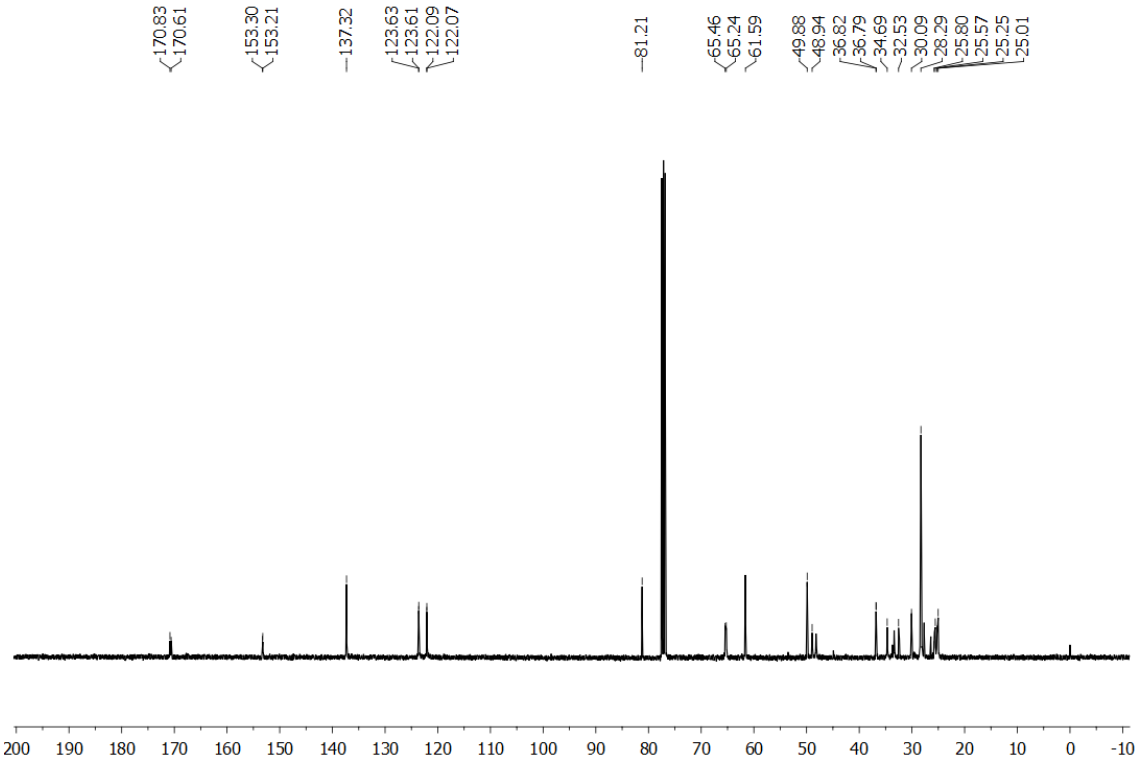

Figure S8. ^{13}C NMR spectrum ($CDCl_3$, 100 MHz) of compound **5b**.

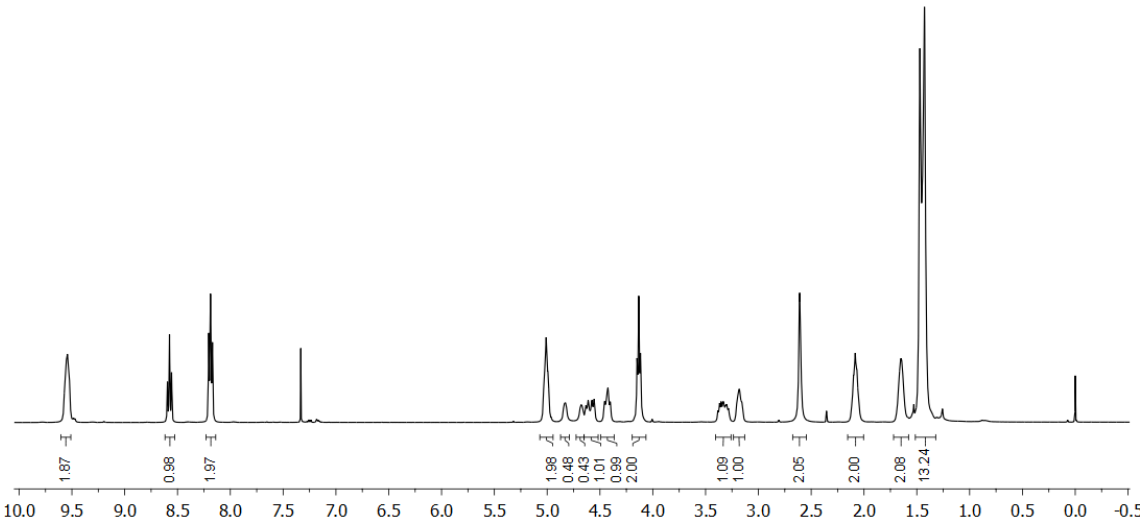

Figure S9. ^{1}H NMR spectrum ($CDCl_3$, 400 MHz) of compound **5c**.

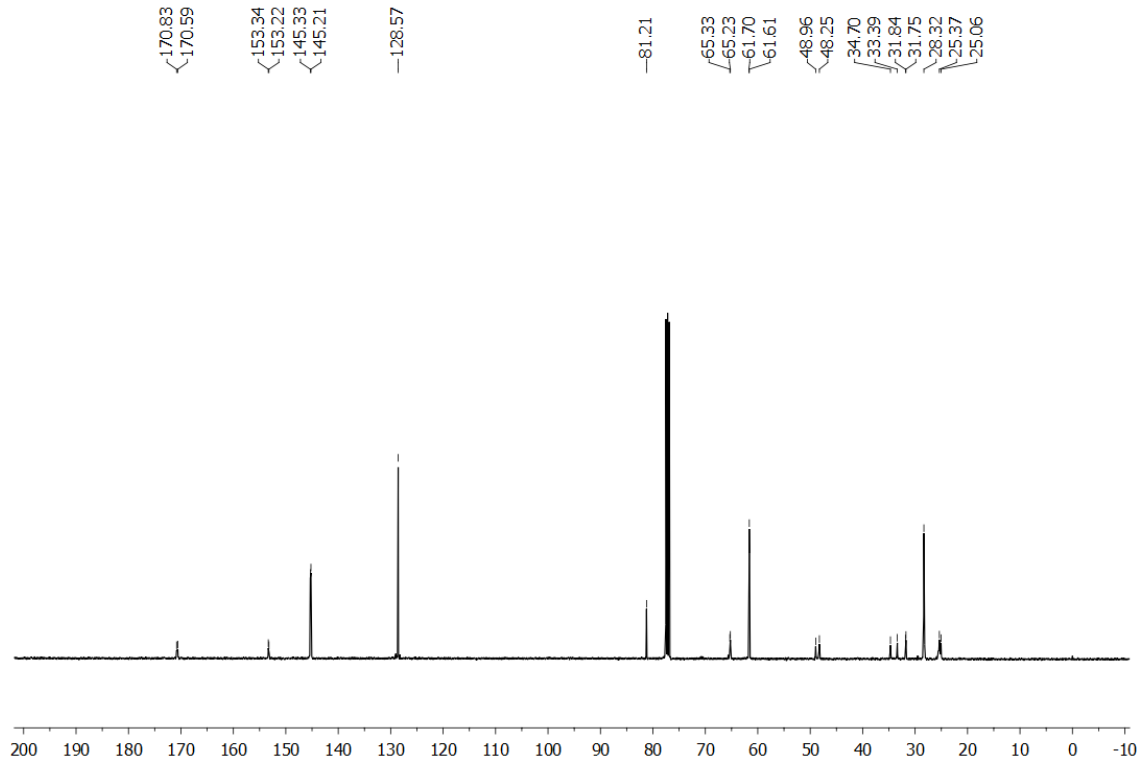

Figure S10. ^{13}C NMR spectrum ($CDCl_3$, 100 MHz) of compound **5c**.

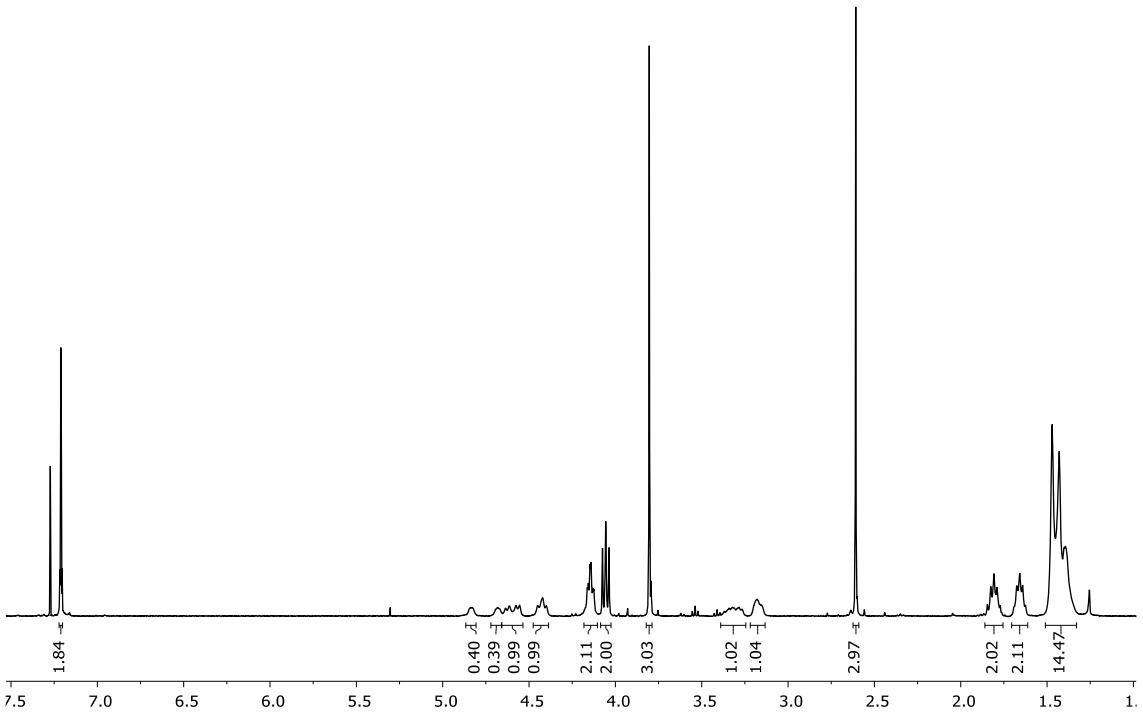

Figure S11. ^{1}H NMR spectrum ($CDCl_3$, 400 MHz) of compound **6a**.

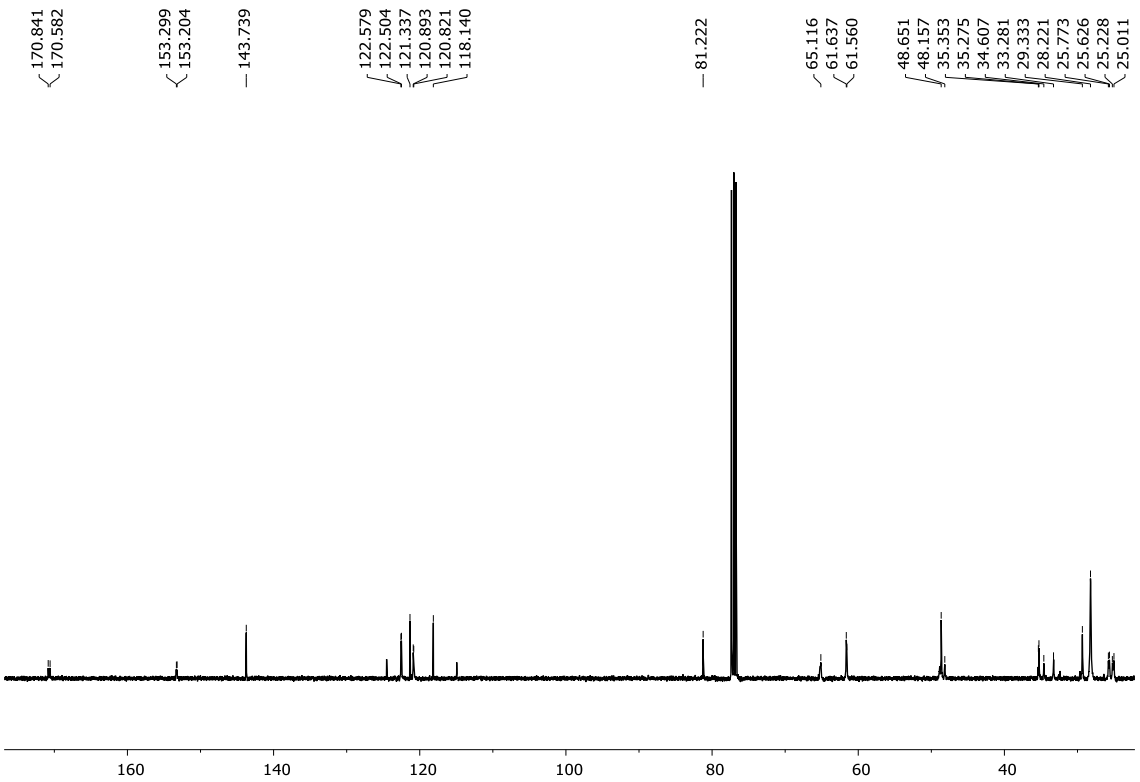

Figure S12. ^{13}C NMR spectrum ($CDCl_3$, 100 MHz) of compound **6a**.

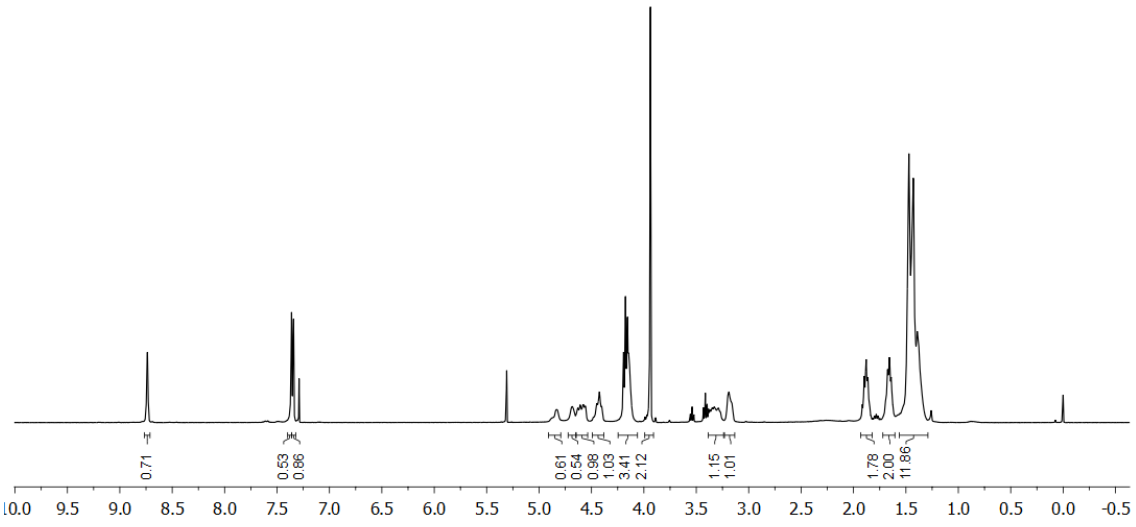

Figure S13. ^{1}H NMR spectrum ($CDCl_3$, 400 MHz) of compound **6b**.

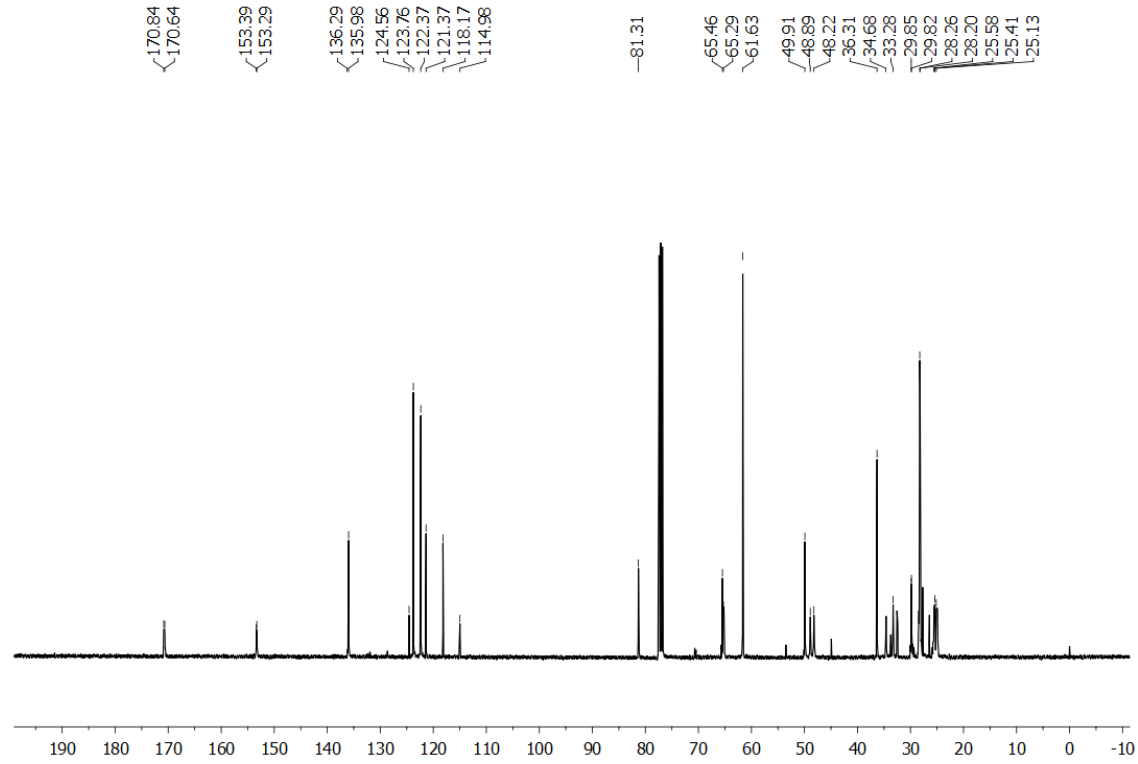

Figure S14. ^{13}C NMR spectrum ($CDCl_3$, 100 MHz) of compound **6b**.

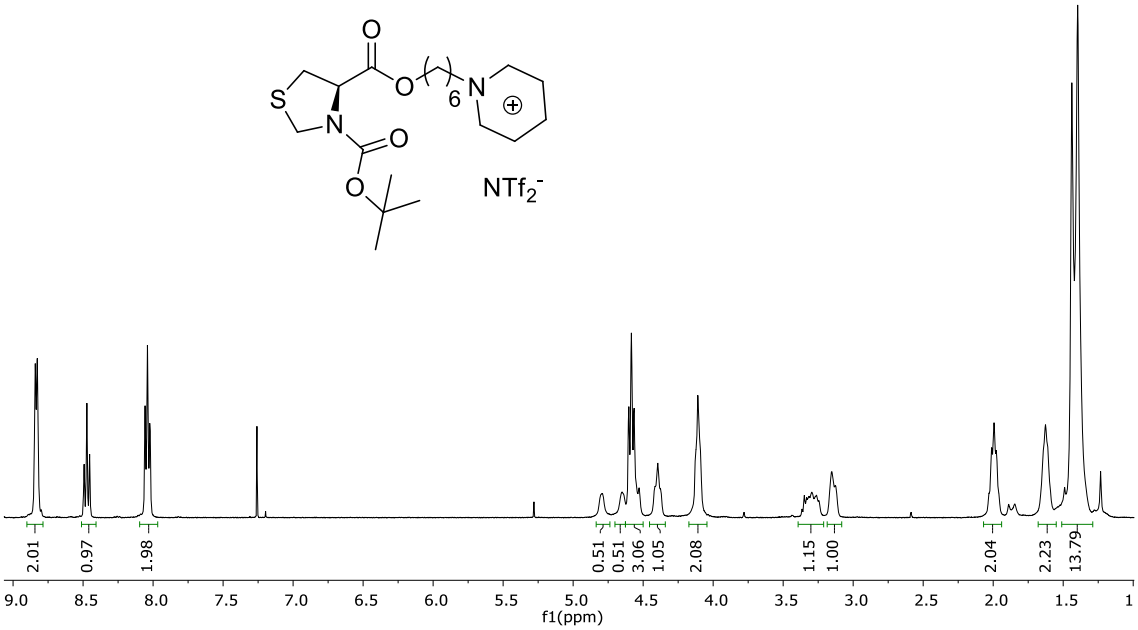

Figure S15. ^{1}H NMR spectrum ($CDCl_3$, 400 MHz) of compound **6c**.

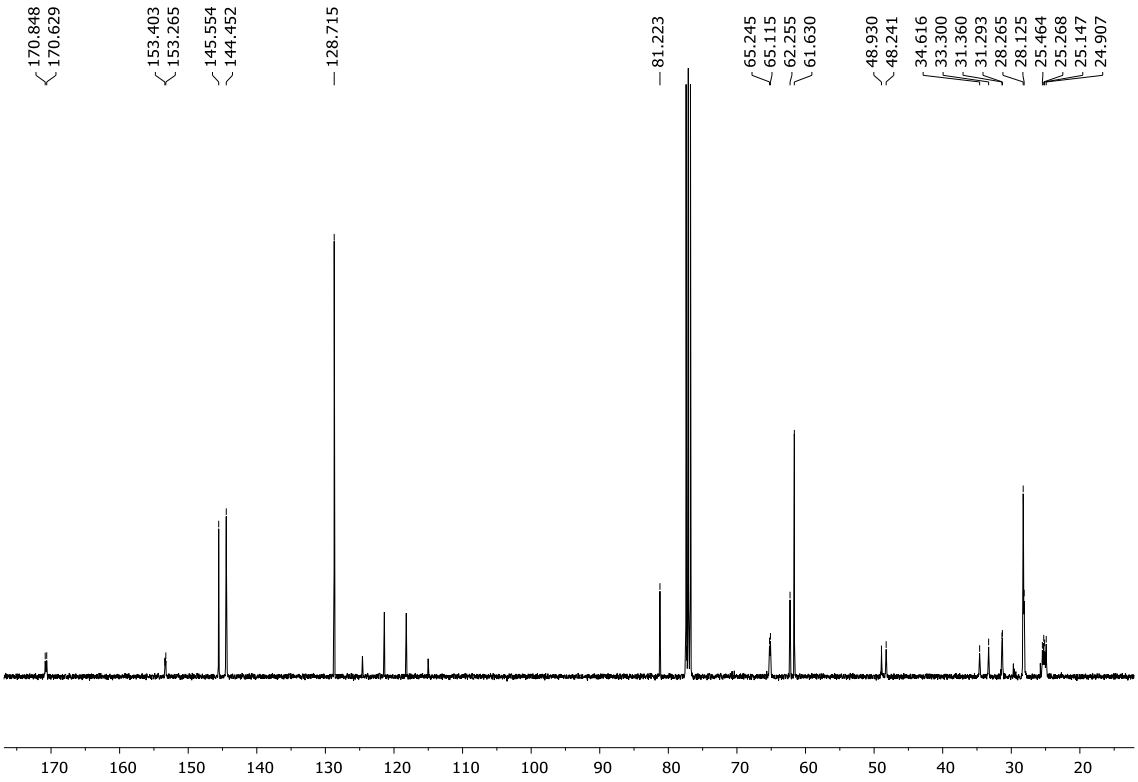

Figure S16. ^{13}C NMR spectrum ($CDCl_3$, 100 MHz) of compound **6c**.

Additional Photophysical Data

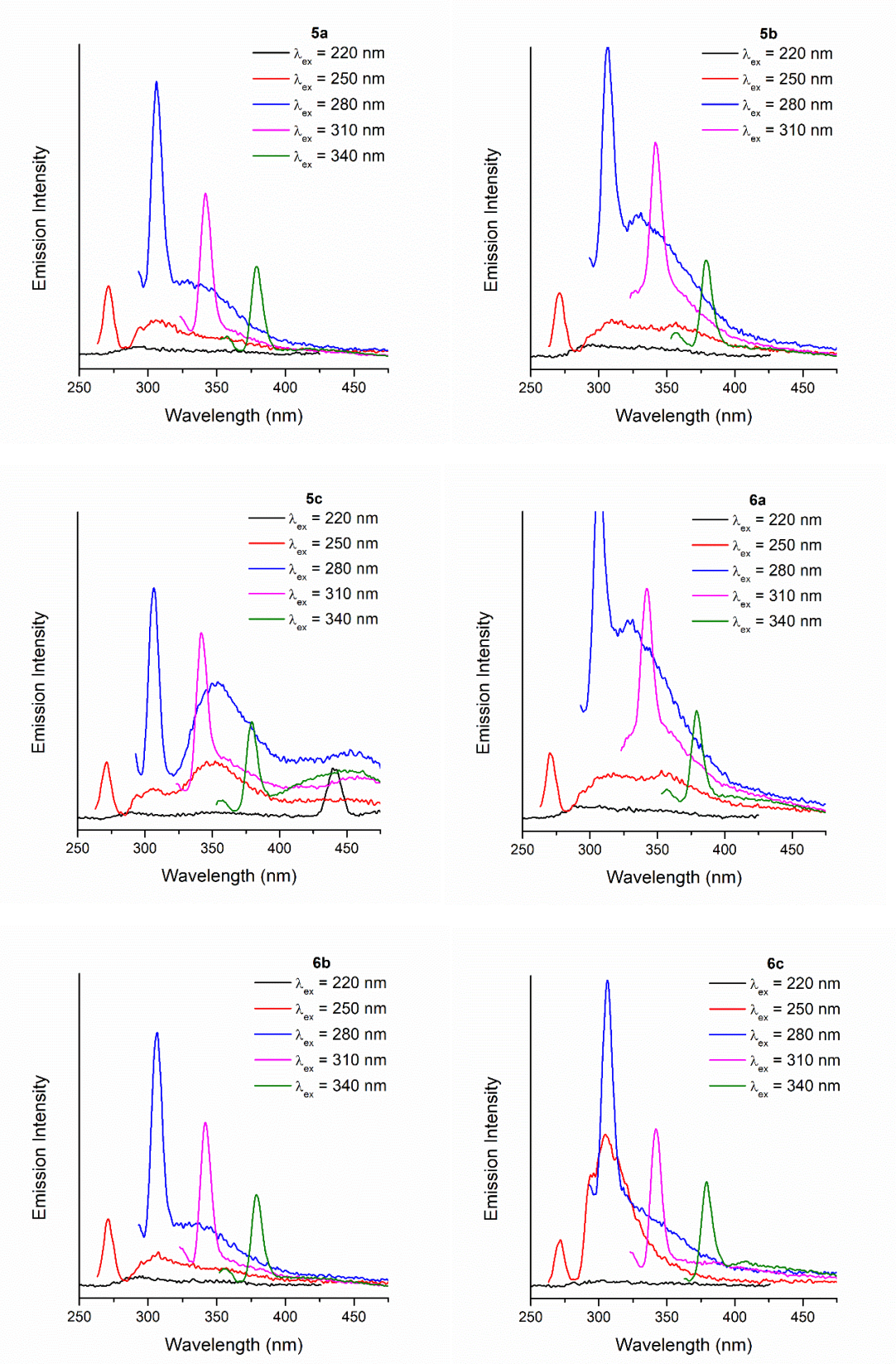

Figure S17. Fluorescence emission spectra of compounds **5a-c** and **6a-c** in ethanol using different excitation wavelengths.

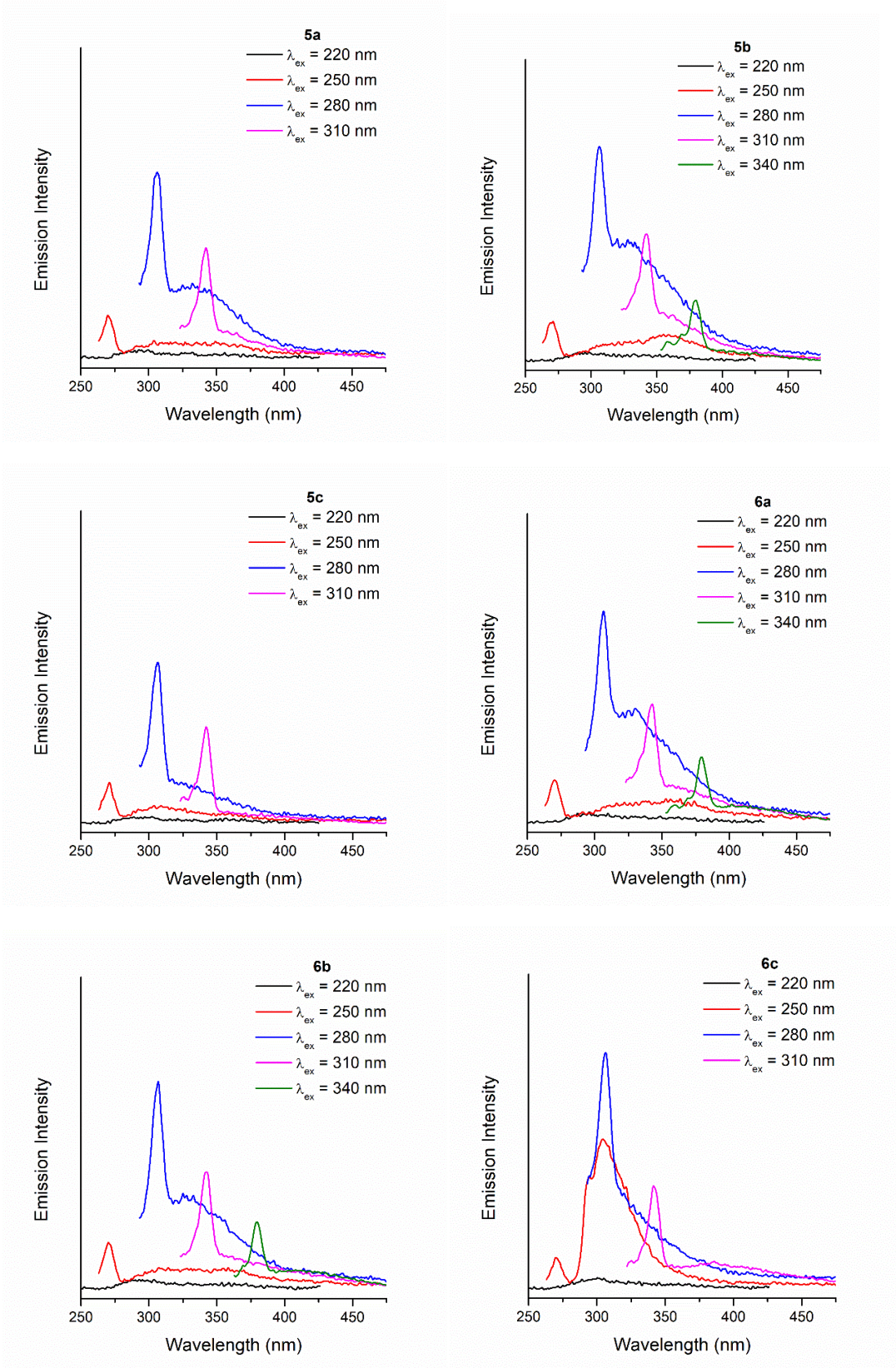

Figure S18. Fluorescence emission spectra of compounds **5a-c** and 6**a-c** in acetonitrile using different excitation wavelengths.

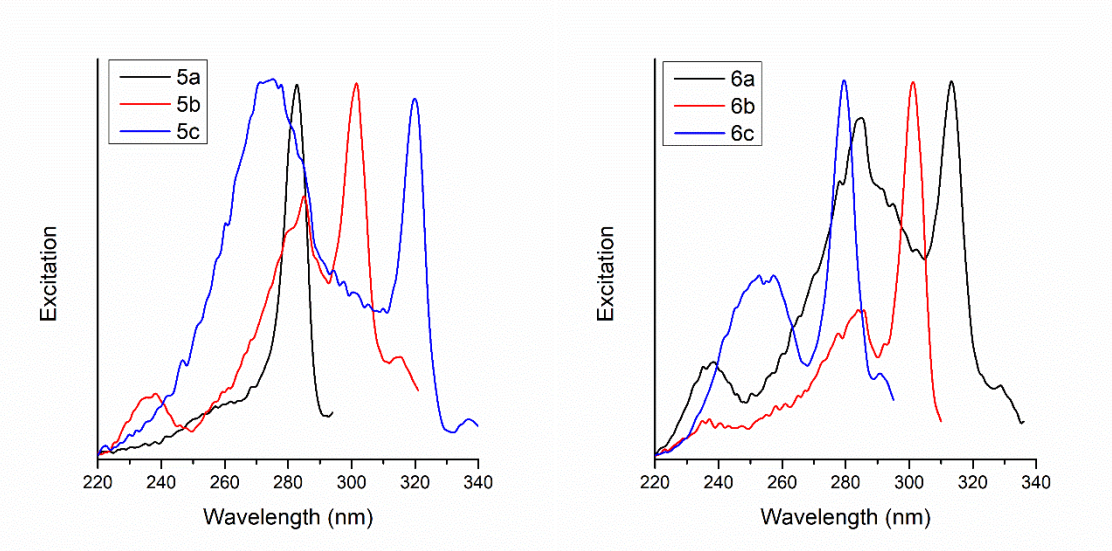

Figure S19. Excitation spectra of **5a-c** (left) and **6a-c** (right) in ethanol.

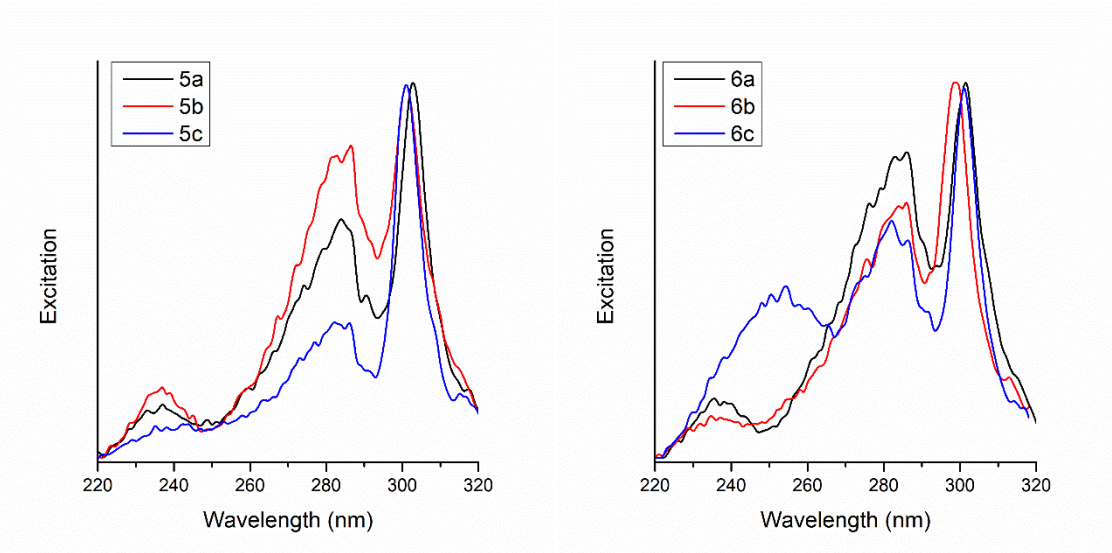

Figure S20. Excitation spectra of **5a-c** (left) and **6a-c** (right) in acetonitrile.

Additional Theoretical Data

Table S1. SAPT2 energy decomposition for a two-body system molecule-bromine.

Measurement	6a (kcal·mol^{-1})	6b (kcal·mol^{-1})	6c (kcal·mol^{-1})
Electrostatics	-102.32	-97.12	-94.45
Exchange	42.17	39.92	41.02
Induction	-19.96	-20.10	-20.43
Dispersion	-19.60	-17.16	-15.39

Table S2. Dipole moments comparison for the fully optimized S_0 and S_1 geometries.

S_1	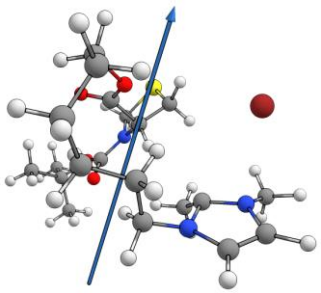	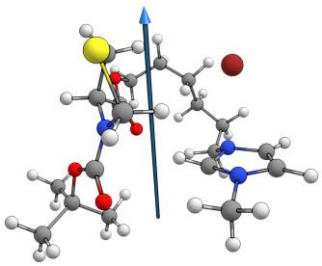	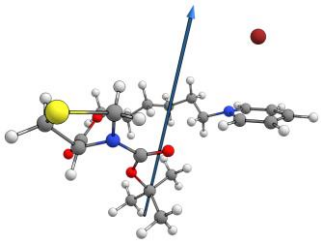
	3.972 Debye	3.729 Debye	4.276 Debye
S_0	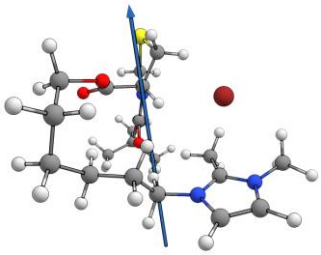	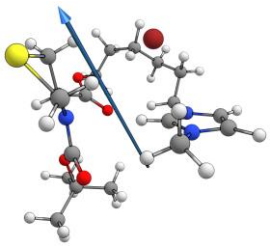	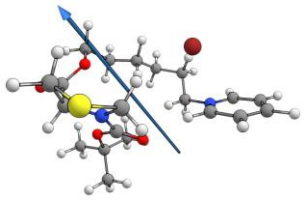
	9.743 Debye	9.269 Debye	9.660 Debye

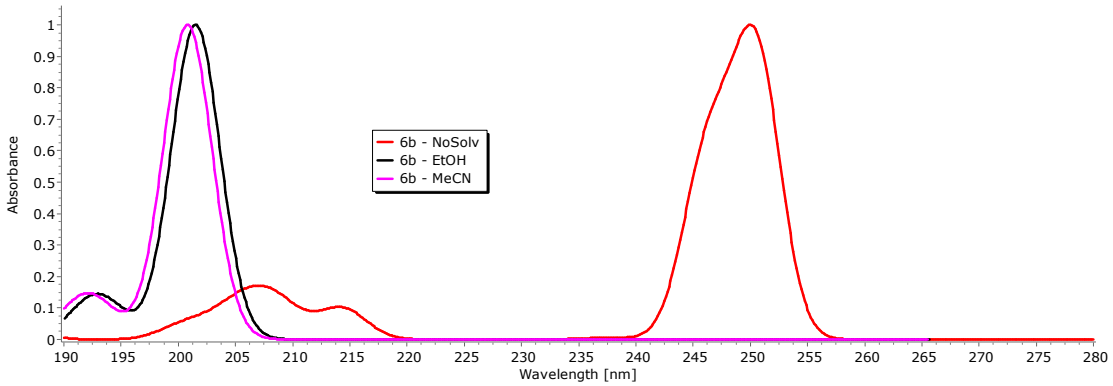

Figure S21. Comparison of the ωB97X-D3/Def2-TZVP absorption spectra for molecule **3b** using no solvation model (red) and CPCM for ethanol (black) and acetonitrile (pink).

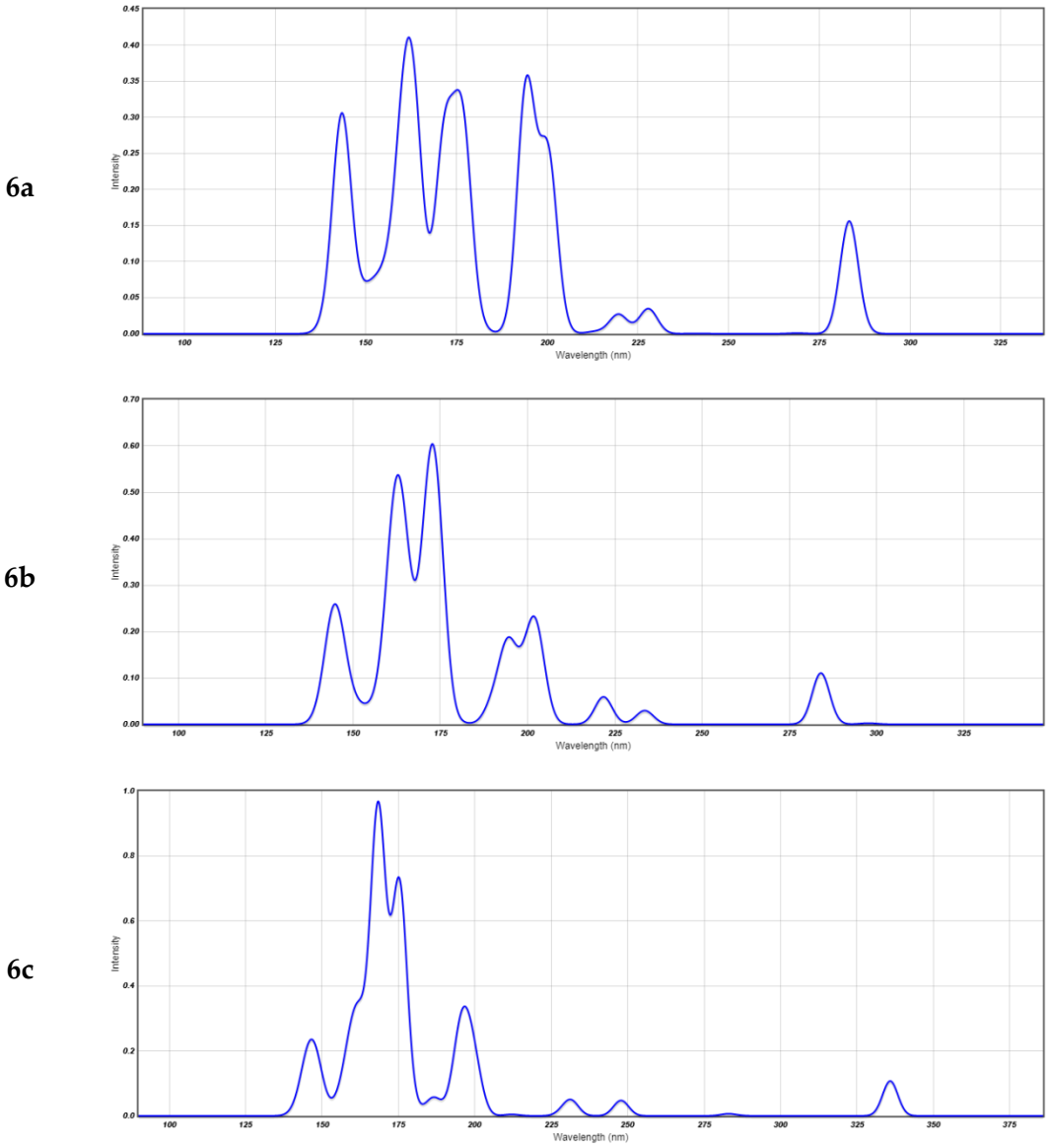

Figure S22. Absorption spectra calculated using CAS(30,15) on the MOPAC software with COSMO solvation to simulate ethanol.

Additional Optical sensing Data

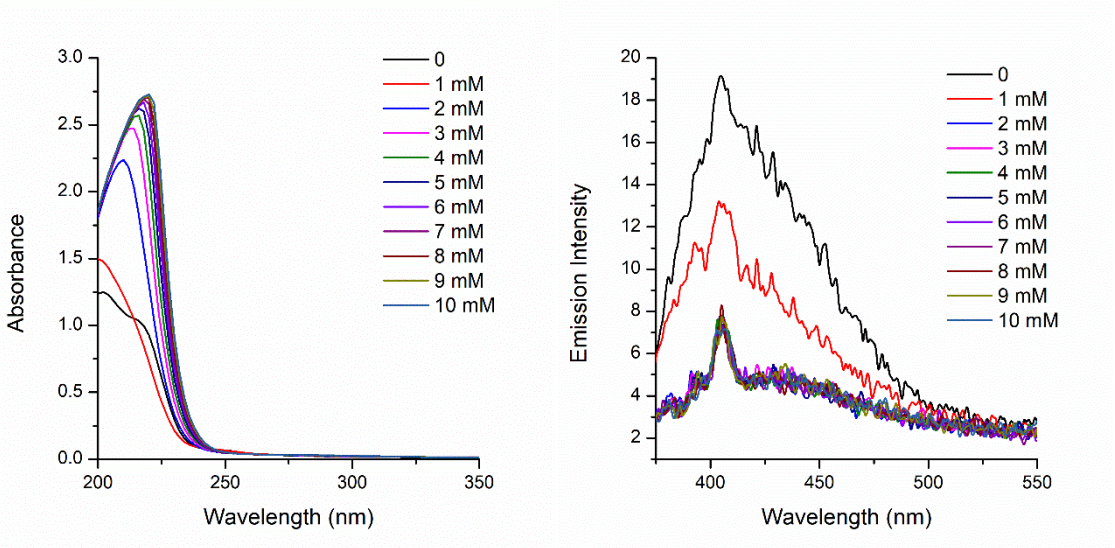

Figure S23. UV-Vis absorption (left) and fluorescence emission (right) spectra of **5a** at different amounts of Zn^{2+} in a CH_3CN/H_2O solution.

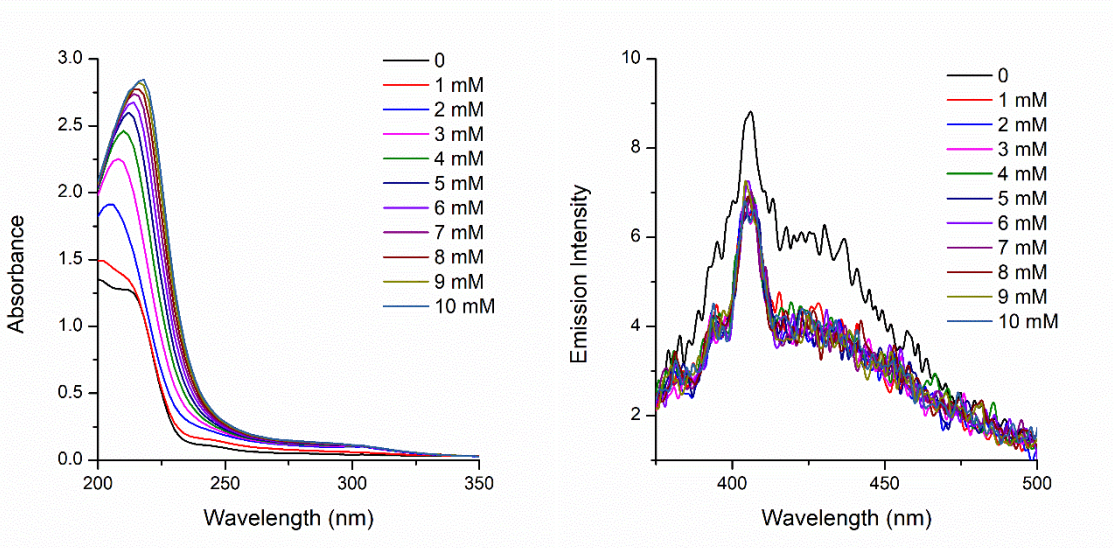

Figure S24. UV-Vis absorption (left) and fluorescence emission (right) spectra of **5a** at different amounts of Co^{2+} in a CH_3CN/H_2O solution.

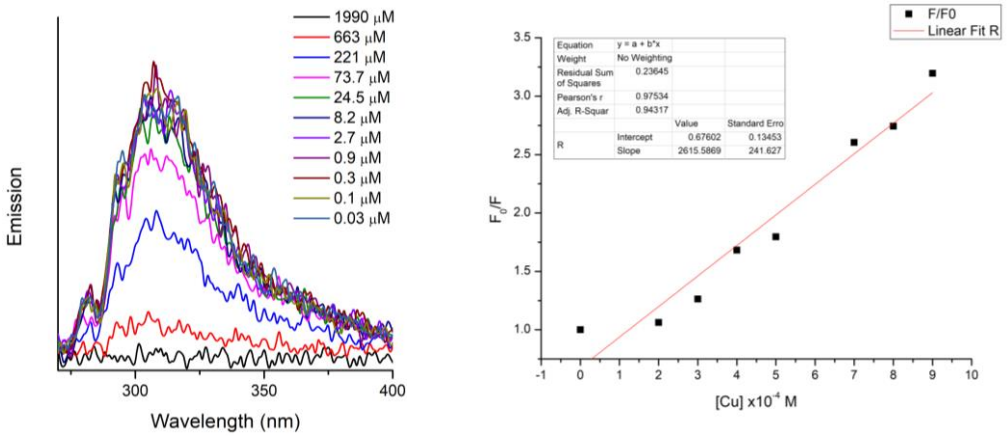

Figure S25. (left) Fluorescence emission spectrum of **5a** at different concentrations of Cu^{2+} in CH_3CN solution and (right) respective Stern-Volmer plot.

Table S3. Binding models for investigation of the interaction between ionic liquid and copper ion from the fluorescence titration data using supramolecular.org.

Metal	**Binding model (Host- guest)**	**K (M^{-1})**	**Error Percentage**
Cu^{2+}	1:1	3565.08	± 3.1247
	2:1	4978.55	± 1.2620
		-4957.18 M^{-1}	± -0.2708
Results for Nelder-Mead (1:1 model): http://app.supramolecular.org/bindfit/view/02c6fe28-e965-417f-af22-c1541f3ccba7			
Results for none Nelder-Mead (full) (2:1 model): http://app.supramolecular.org/bindfit/view/ada49cc1-7bdb-4737-81ec-b875fec623e6			